Concentrated load introduction in CLT elements perpendicular to plane

Bogensperger Thomas, Competence Center for Timber Engineering – holz.bau forschungs gmbh, A-8010 Graz, bogensperger@tugraz.at

Jöbstl Robert August, Haas Fertigbau Holzbauwerk GmbH & Co KG/Haas Holzprodukte GmbH, Radersdorf 62, A-8263 Großwilfersdorf /Industriestraße 8, D-84326 Falkenberg, robert.joebstl@haas-group.com

Keywords:

Cross laminated timber (CLT), concentrated load introduction, column supported CLT slab, punching strength

1 Introduction

Cross laminated Timber (CLT) – also known as X-lam – can be utilised as a plate-like element for loads in and/or out of plane. Under loads out of plane bending moment and shear force develop often in one direction. For this cases several methods for computation of internal section forces are available. For example the well known Timoshenko beam theory, which takes into account the high weakness of layers under rolling shear stresses is one commonly used representative. Other methods are e. g. the modified γ-method and the shear analogy method [8, 9]. A recently work out study [1] showed that differences in the calculation of stresses determined with higher theories and simple beam theories like Timoshenko's are negligible.

Modern challenging architecture is demanding solutions where CLT slabs activate two dimensional load carrying behaviour. Support by columns (e.g. see Fig. 1.1) is often needed for such solutions. For this purpose plate theories under consideration of shear effects (better known as Reissner-Mindlin-plate theory) are a de-facto standard for the computation of stresses. The mechanical stiffness properties for the Reissner-Mindlin plate theory can be found in [2]. Usually five stiffness values – two bending, one twist and two shear stiffness values – are necessary. Typically the distribution of internal section forces and moments of CLT elements under concentrated loads show high values in a small zone around the load. It this context it has to be mentioned that strength verifications for CLT elements are widely clear for internal section forces and moments except twisting moments [3].

Reissner-Mindlin plate theory corresponds to Timoshenko beam theory, but comparably 2D plate-theories on comparable level of modified γ-method or shear analogy

method, implemented e.g. in FEM software for engineering applications, are still missing.

Figure 1.1. examples for CLT plates with column support.

This paper deals with bending and shear failure of cross laminated timber (CLT) plates under concentrated loads generated by e.g. columns as supports. Several verifications have to be performed for this cases: One is the verification of compression perpendicular to plane (presented by Bogensperger et. al at CIB meeting in 2011 [10]). In addition the bending and shear stresses in the CLT plate under high local loads (punching) have to be done which shall be presented in this paper.

2 State of the art

Bending verifications of CLT panels have to consider effective cross section properties due to the orthogonally layered cross-section the of CLT panels. A typical CLT cross section is shown in Fig. 2.1.(a) and has a typical stress distribution like a "saw blade". Strength properties are based on tension strength values of the graded timber boards used for the production. A model, which links tension strength values of graded timber boards to the CLT bending strength values was presented in [6]. For the application in practise the proposed formula is often simplified in a form $f_{mk,CLT}=\alpha \cdot f_{mk,g,0}$ with α = 1,1 to 1,2 and $f_{mk,g,0}$ as bending strength of comparable glulam. This formula can be found in most of the approvals of relevant CLT producers.

Typical shear stress distribution can be seen in Fig. 2.1.b. The maximum shear stress occurs at the centre of gravity of the underlying cross section. Shear verification has to consider the corresponding strength values of each layer. In layers where rolling shear stresses develop shear stress distribution is almost constant and the crucial location of the rolling shear verification can be found in that layer, which is next to the centre of gravity. The relevant rolling shear strength $f_{v,90,k,CLT}$ can be assumed with 1,25 N/mm² if grooves in the lamellas are absent and geometric ratio of used lamellas fulfils ratio of $b/t \geq 4$ (b ... width and t ... thickness of the board).

P. Mestek [5, 11] investigated shear respectively punching resistance of CLT elements under uniformly distributed and high concentrated loads. The used test con-

figuration is shown in Fig. 2.2. The measurements of the tested CLT elements was chosen with 1380/1020 mm which were simple supported at all four sides. The CLT section was a 7-layered element with an overall thickness of 189 mm. Based on these geometrics a span to thickness ration of $L/t_{CLT} \approx \sqrt{a \cdot b}/t_{CLT} = \sqrt{1380 \cdot 1020}/189 = 6,28$ can be estimated. The work of Mestek focused on the improvement of shear and punching resistance by the application of self tapping screws drilled into the slab under 45° closed to the local load introduction. CLT panels were investigated which were built up with grooves in the lamellas. As a disadvantage of these grooves the rolling shear strength is significantly reduced. Therefore a reinforcement with self tapping screws is a meaningful approach for such CLT panels whereas the research presented in the following is concentrated on the resistance of CLT panels without screws in CLT panels (except for the local load introduction with screws under 90° of the layers).

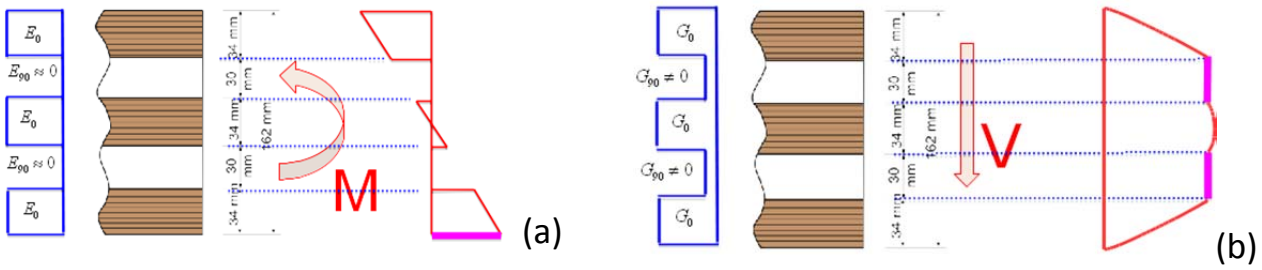

Figure 2.1. (a) typical bending stress distibution in CLT; (b) typical shear stress distibution in CLT

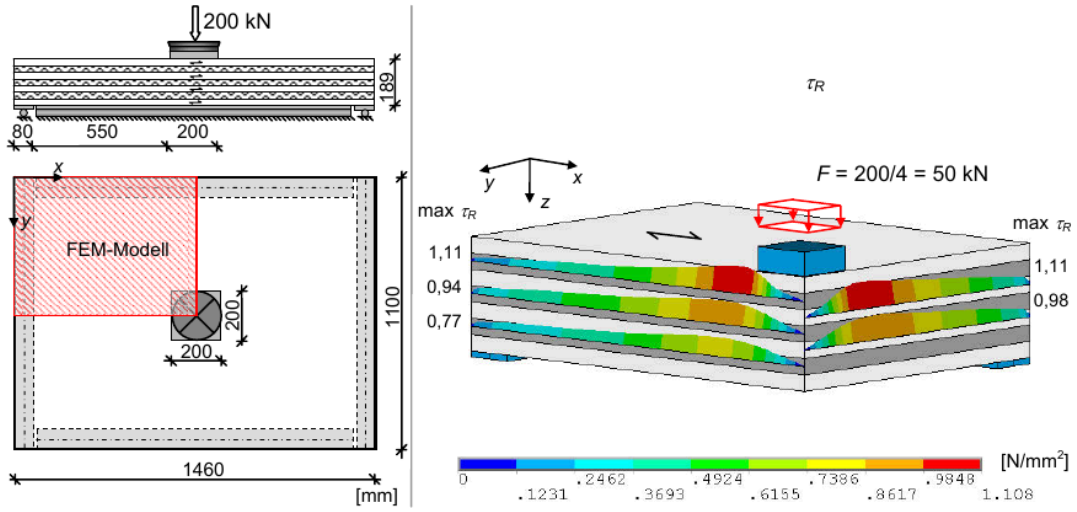

Figure 2.2. Test configuration used by Mestek [5, 11]

Although Mestek investigated primarily the effect of a reinforcement with screws in CLT elements, some tests without 45° screws were conducted (Fig. 2.3.a). CLT elements with grooves in lamellas were used. Additional tests were carried out which compare the rolling shear strength of lamellas with and without grooves. Based on these results a rolling shear strength for CLT panels built-up with lamellas without grooves could be estimated between 2,06 to 2,25 N/mm². It has to be mentioned that the verification of the rolling shear was performed along a controlling perimeter line or – written in terms of Mestek – along the intersection line (Fig. 2.3.b).

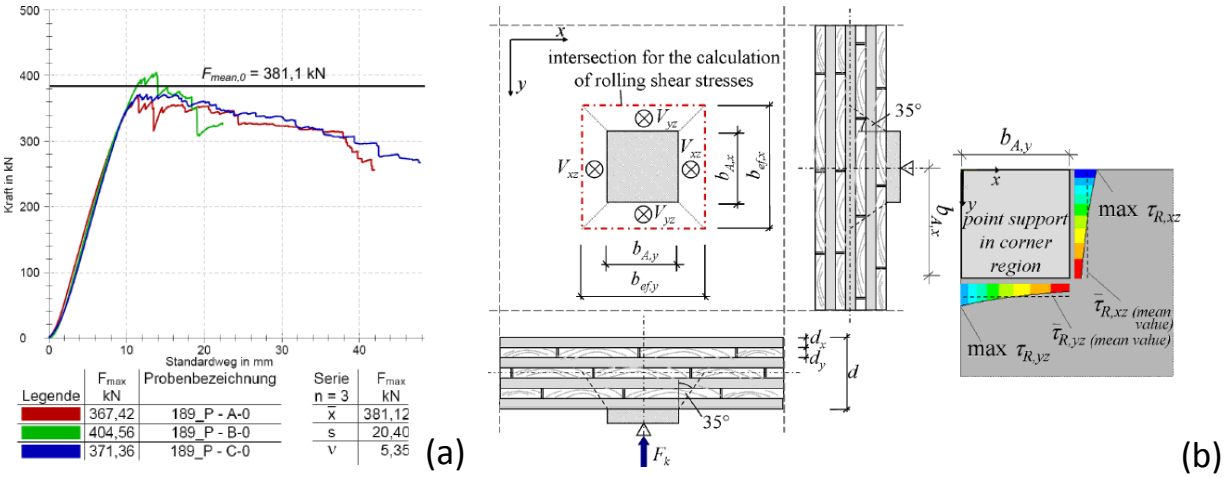

Figure 2.3. (a) Test results of Mestek without reinforcements with selftapping screws (b) controlling perimeter for shear stresses [5, 11]

3 Numerical studies

The dominating failure mechanism (bending, shear) of CLT plates under a concentrated load depends primarily on the geometric dimensions of the CLT plate (mean span to thickness $\sqrt{(a \cdot b)}/t_{CLT}$, ratio a/b of spans in *x* and *y* direction and the number of layers and the relation of thickness of adjacent layers).

These parameters were investigated numerically by means of FEM in combination with strength verifications based on the findings mentioned in Cap. 2. In a first step the optimum a/*b* ratio (Fig. 3.1.a) was evaluated under the constraint condition that the total area of the CLT plate should remain $a \cdot b$=1 m² and under consideration that the rolling shear stresses should be the same for both directions *x* and *y*. The rolling shear verification was carried out in the controlling perimeter line around the load introduction. This controlling perimeter line was computed under an assumed load spreading angle of 35° according to Mestek (Fig 3.1).

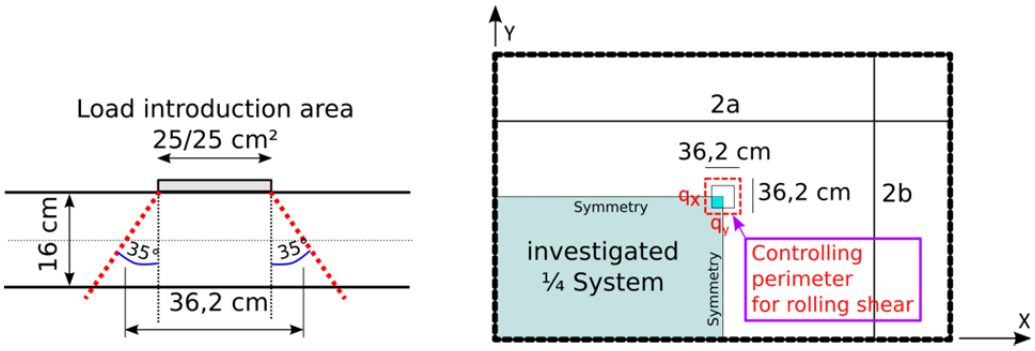

Figure 3.1. controlling perimeter line based on the findings of Mestek

This study was carried out with a 5- and 7- layered CLT cross section. The thickness ratio of adjacent layers was 1:1 and 2:1 respectively. Based on symmetry conditions only ¼ of the system was modelled as illustrated in Fig. 3.1 and Fig. 3.2.a (blue shadowed area). The overall thickness of the CLT panel was chosen with 160 mm (Fig. 3.2.b).

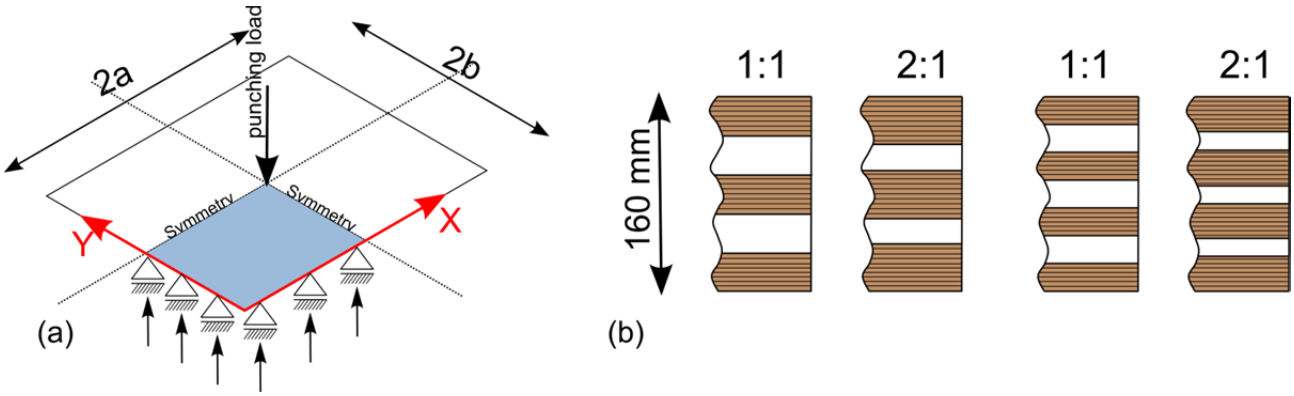

Figure 3.2. (a) variation of a/b *(b) investigated CLT sections worked-out FEM study*

The results with optimised 2·a and 2·b values are summarized in Table 1. One conclusion of the done study is that 5-layered CLT element with equal lamella thickness does not behave well under two dimensional load transfer as an extraordinary *a*/*b* ratio of 50,7/197,3 is the optimum with same rolling shear stress level in both directions. 7-layered CLT element behaves much better with the optimum *a*/*b* ratio of 105,6/94,7=1,11 which is close to a quadratic shape.

Table 1. optimum span length 2·a and 2·b

	2·a [cm]	2·b [cm]
BSP5s_160mm_1:1	50,7	197,3
BSP5s_160mm_2:1	106,1	94,3
BSP7s_160mm_1:1	105,6	94,7
BSP7s_160mm_2:1	161,1	62,1

The *a*/*b* ratio (Mestek chose 138/102=1,35 in his work) differs from results of this study. One important reason lies in the differences of the numerical model: In the present study a 2D shell model was used while Mestek used a 3D solid model.

An other approach for a further study is to investigate differences of expected load carrying capacities under deviating *a*/*b* ratios. Proposed *a*/*b* ratios for a second study are shown in Fig. 3.3.

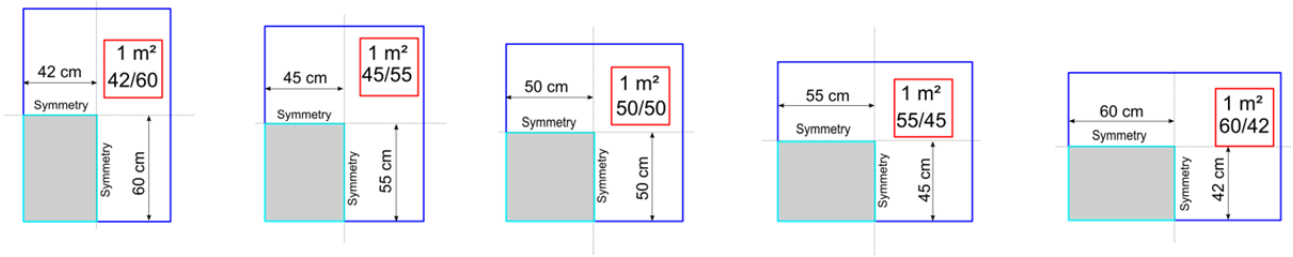

Figure 3.3. investigated a/b ratios

Results of computed FEM-load carrying capacities are illustrated in Fig. 3.4. Based on these it can be concluded, that the a/b ratio of the CLT elements is not as dominant as expected.

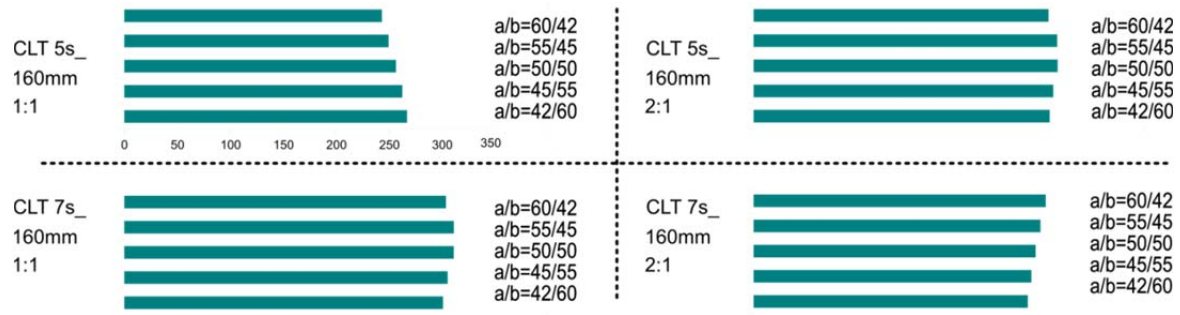

Figure 3.4. expected load carrying capacities for different a/b ratios based on a FEM-study

4 Development of test configuration

Test specimens for the tests presented in the following should contain 5- and 7-layered CLT elements. Furthermore the chosen cross sections should be available as industrially produced elements. The geometric as wells as stiffness values of the selected cross sections are summarized in table 2. Specimens denoted as "CLT 5s" and "CLT 7s" were delivered from producer 1 while the specimen of series "CLT 7s*" originated from a different producer 2.

Table 2. CLT cross sections used for experimental investigations

	E_0	E_{90}	G_0	G_{90}	#	t_1	t_2	t_3	t_4	t_5	t_6	t_7
	N/mm²	N/mm²	N/mm²	N/mm²		mm	mm	mm	mm	mm	Mm	mm
CLT 5s	11600	≈0	690	50	5	34	30	34	30	34		
CLT 7s	11600	≈0	690	50	7	19	30	19	30	19	30	19
CLT 7s*	11600	≈0	690	50	7	20	30	20	30	20	30	20

A graphical illustration of "CLT 5s" and "CLT 7s" and associated stress distributions for unit section moments and shear forces in longitudinal (0°) and in transverse direction (90°) (m_x=m_y=1 kN·cm/cm, q_x=q_y=1 kN/cm) is given in Fig 4.1.

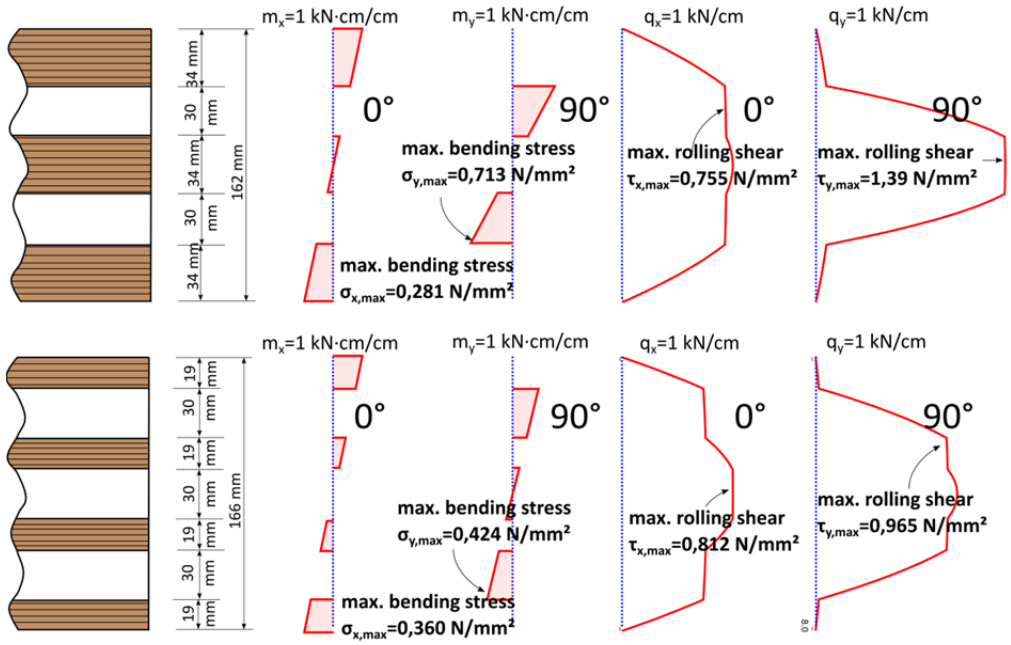

Figure 4.1. CLT cross sections used for experimental investigations and shear stress distributions

A sketch of the test configuration “punching” (test configuration 1) can be found in Fig. 4.2. Ratio of a/b was chosen with 1,0 (a = b = 1,0 m). The supports were implemented by means of tension rods which could be constraint within an existing grid of load introduction points with a distance of 50/50 cm in the laboratory. The span to thickness ratio varied between 6,17 and 5,88 depending on the cross-section. The geometric boundary conditions were thereby similar to the mean span to thickness ratio of Mestek configuration with 6,28. Three images of test configuration 1 are shown in Fig. 4.3.

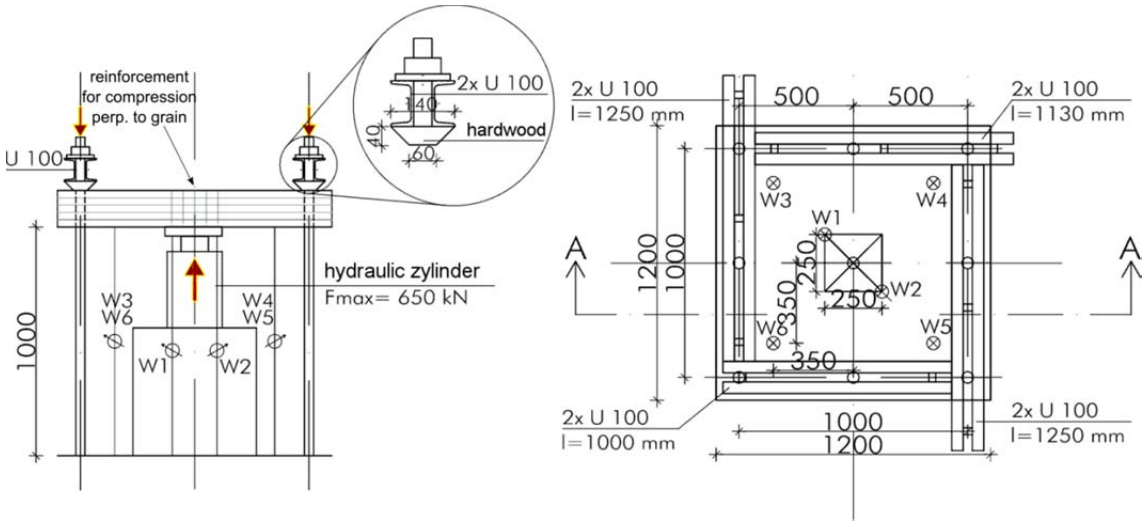

Figure 4.2. Test configuration for expected punching shear failure (test configuration 1)

Figure 4.3. Images of test configuration for expected punching shear failure (test configuration 1)

The test configuration “bending under concentrated loads” were designed with significant higher length to thickness ratio in order to achieve bending failure modes (test configuration 2). Restricted to the grid of load introduction points of the test field the longer span a was chosen with 4,0 m, the shorter span b with 2,5 m. Mean length to thickness ratios were between 19,5 and 18,6 depending on the used cross section. As the parameter study already showed that 5-layered CLT elements behave worse than 7-layered ones under all side support with global bidirectional bending behaviour. Therefore tests with one directional bending behaviour with support only along both shorter sides was proposed for 5-layered CLT elements while a two directional bending loading (with simple supports on all four sides) of the CLT elements was implemented for the 7-layered CLT element (Fig. 4.4).

Test specimens denoted with “A” are build up in the laboratory for series "CLT 5s" and "CLT 7s". The lamellas used were graded in respect to density of the boards within a range of 400 kg/m³ ± 20 kg/m³. Annual ring pattern was the second grading parameter. The allowance of knots was reduced in comparison to industrially graded boards. Test specimens with CLT elements from producer 1 are denoted with “B”. If they came from producer 2 they are denoted as series “C”.

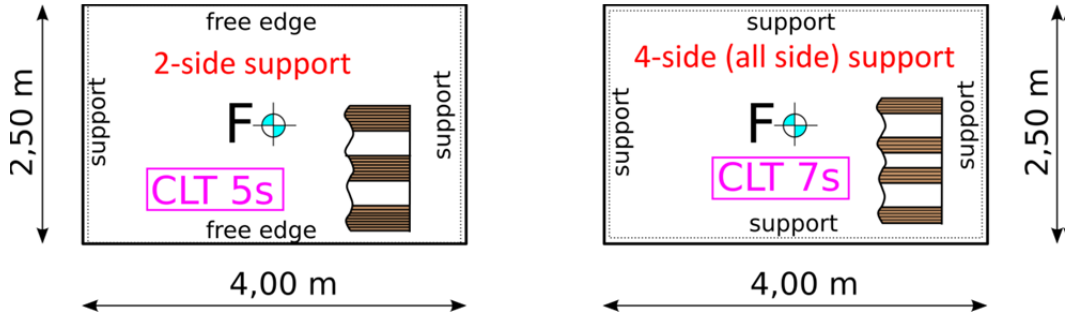

Figure 4.4. Test specimens for expected bending failure (test configuration 2)

Two images of test configuration 2 can be found in Fig. 4.5.

Figure 4.5. Images of test configuration 2 for test series with expected bending failure mode

5 Test results

The load-displacement curves of the tested showed a relative ductile behaviour for test configuration 1 (Fig 5.1) Different failure modes were observed. The non linear characteristic indicates an increasing loss of shear strength which is more or less a relative steady process. In some cases failure modes of lamellas in tension in conjunction with unsteady load-displacement curves was observed.

For specimens of test configuration 2 bending failure always occurred first. Subsequently rolling shear failures were observed. A ductile behaviour could be recognised also for test configuration 2 (Fig 5.2). As failure of several lamellas in tension leaded to an immediate load decrease discontinuities in the load displacement curve were developed more significant in configuration 2 than 1, especially in case of the tests with 5-layered CLT elements.

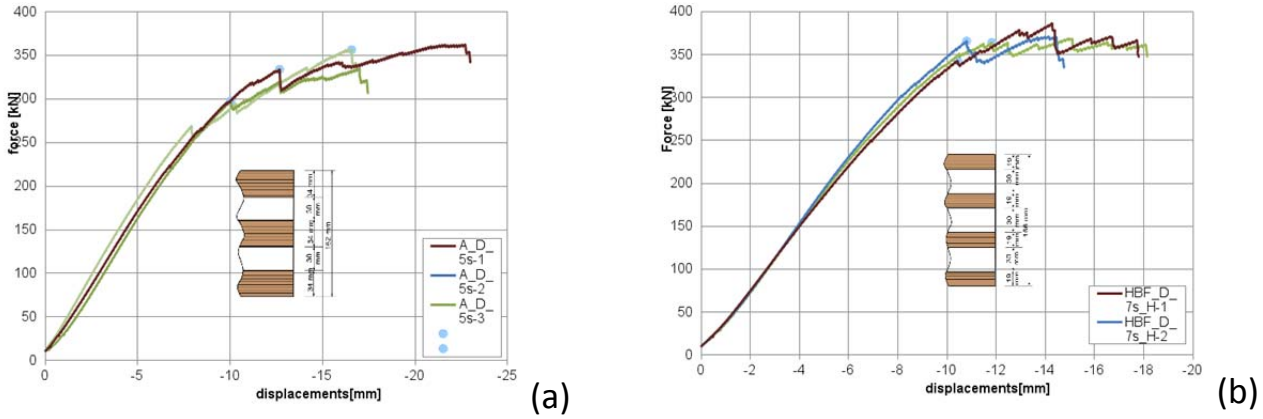

Figure 5.1. load displacement curves (a) 5-layered CLT; (b) 7-layered CLT in test configuration 1

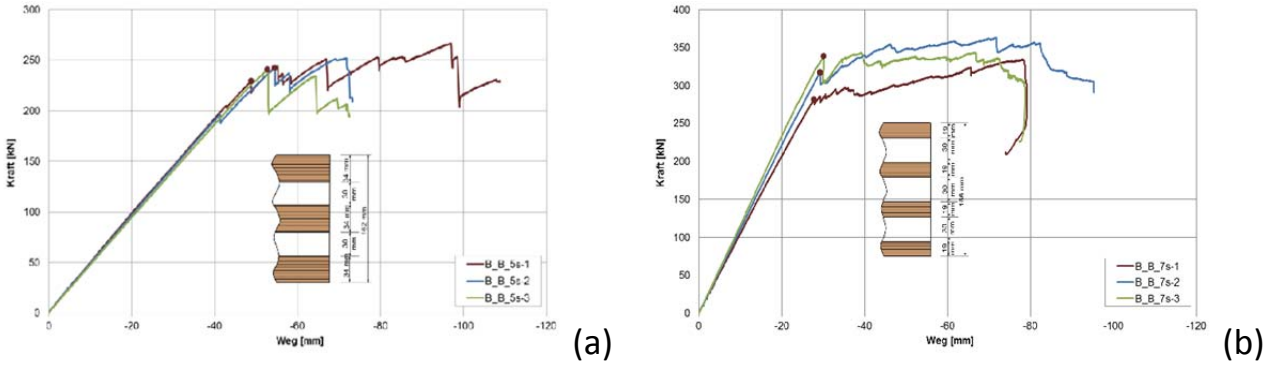

Figure 5.2. load displacement curves (a) 5-layered CLT; (b) 7-layered CLT in test configuration 2

Failure of lamellas under tension was also observed in configuration 1. But the already established non linear character of the load displacement curve indicates already existing failures due to shear, whereas in configuration 2 unsteadiness always finishes the linear load displacement behaviour.

Typical shear failures are shown in figure 5.3. These failures became visible by cuting the test elements along their axis of symmetry after the tests. In the area of the load introduction could be easily detected due to indentations of the steel plate and the used reinforcement screws.

Figure 5.2. observed typical failures in test configuration 1

Figure 5.4 shows typical failures observed in test configuration 2. In the first row failures of 5-layered bending under more or less one dimensional bending could be

detected whereas the images in the second row show impressive destruction under pure two dimensional bending for the 7-layered CLT specimens.

Figure 5.3. observed typical failures in test configuration 2

All numerical results concerning test configuration 1 can be found in table 3, in an analogous manner table 4 contains the test data of test configuration 2.

Table 3. Test results of test configuration 1

Typ of CLT panel			5-layered CLT panels		7layered CLT panels		
Identification of test series			A_D-5s	B_D-5s	A_D-7s	B_D-7s	C_D-7s
Width of lamellas b	Longitudinal lay.	[mm]	235	230	235	230	181 (90)[1)]
	Cross layer	[mm]	120	190/120	120	190	184 (90)[1)]
Thickness of boards h	Longitudinal lay.	[mm]	34	34	19	19	20
	Cross layer	[mm]	30	30	30	30	30
ratio b/h	Longitudinal lay.	[-]	6,91	6,76	12,4	12,1	9,05 (4,50)[1)]
	Cross layer	[-]	4,00	6,33/4,00	4,00	6,33	6,13 (3,00)[1)]
Number of test specimens (in evaluation)		[-]	6	4	6	3	4
Moisture content u	Mean value	[%]	11,7	11,3	12,1	10,0	11,0
	COV	[%]	6,40	9,90	5,88	1,33	3,06
density ρ	Mean value	[kg/m³]	414	435	412	460	431
	COV	[%]	4,13	5,03	5,46	5,20	6,60

stiffness	Mean value	[kN/mm]	35,4	32,2	39,0	42,8	42,6
	COV	[%]	4,28	3,80	4,40	7,29	6,90
Force level at first crack $F_{1.\ crack}$	Mean value	[kN]	328	289	350	(400)[2)]	351
	COV	[%]	6,90	5,76	4,17	(7,08)[2)]	9,42
	5%-Quantile NV	[kN]	291	262	326	(353)[2)]	296
	charact. value acc. to EN 14358	[kN]	279	247	311	(320)[2)]	273
Maximum of load F_{max}	Mean value	[kN]	358	339	372	(408)[2)]	366
	COV	[%]	3,87	3,72	2,04	(4,70)[2)]	5,85
	5%-Quantile NV	[kN]	335	318	360	(376)[2)]	331
	charact. value acc. to EN 14358	[kN]	318	296	331	(348)[2)]	313

Remarks:
1) Values in brackets represent ratios of b/t under consideration of grooves.
2) Appropriate values of series B_D-7s represent bending failure.

Table 4. Test results of test configuration 2

Typ of CLT panel			5-layered CLT panels	7-layered CLT panels, support at all sides	
Identification of test series			B_B-5s	B_B-7s	C_B-7s
Number of test specimens		[-]	3	3	3
Moisture content u	Mean value	[%]	10,7	9,70	10,8
	COV	[%]	4,07	9,54	2,45
density ρ	Mean value	[kg/m³]	442	440	445
	COV	[%]	10,8	4,48	2,72
stiffness	Mean value	[kN/mm]	4,78	11,0	11,2
	COV	[%]	1,85	5,12	2,15
Force level at first crack $F_{1.crack}$	Mean value	[kN]	238	312	361
	COV	[%]	3,03	9,18	8,09
	5%-Quantile NV	[kN]	226	265	313
	charact. value acc. to EN 14358	[kN]	203	232	280
Maximum of load F_{max}	Mean value	[kN]	253	347	369
	COV	[%]	5,10	4,25	5,84
	5%-Quantile NV	[kN]	232	323	333
	charact. value acc. to EN 14358	[kN]	216	296	314

6 Recommendations for standardisation

The results of test configuration 1 serve as basis for punching shear strength values. Rolling shear strength values are evaluated with the maximum of elastic shear forces q_x and q_y along the controlling perimeter line (see Fig. 3.1). The test results of series C (producer 2) are exceptional as lamellas of this series contains grooves. These grooves are essentially smaller than those in [5]. A graphical comparison shows the differences of the grooves in [5] and the present study (Fig. 6.1).

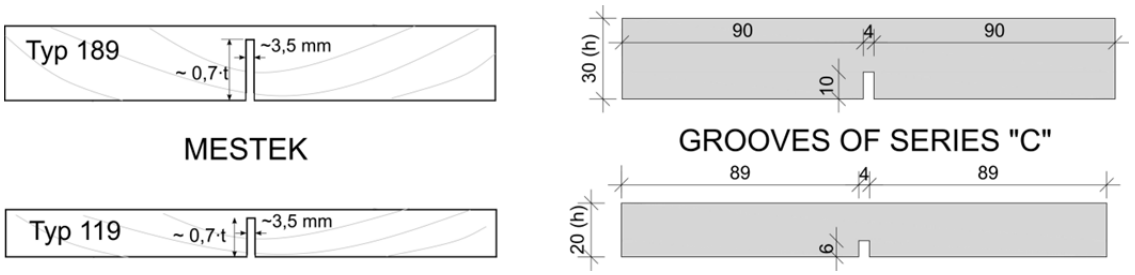

Figure 6.1. differences between grooves in Mestek [5] and test specimens of the presented tests

Based on forces defined at first crack level (see table 3) the associated stress values for rolling shear could be identified and values are summarized in table 5.

Table 5. rolling shear strength values (based on results of configuration 1)

Typ of panel	5-layered CLT panel		7-layered CLT panel		
Identification of test series	A_D_5s	B_D_5s	A_D_7s	B_D_7s	C_D_7s
charact. value (EN 14358)	279	247	311	320	273
$q_{x,max}$ [kN/cm]	2,74	2,43	2,37	2,44	2,08
$q_{y,max}$ [kN/cm]	1,59	1,41	2,40	2,47	2,10
rolling shear str. $\tau_{90,x}$ [N/mm²]	2,07	1,83	1,92	1,98	1,69
rolling shear str. $\tau_{90,y}$ [N/mm²]	**2,21**	**1,95**$^{*)}$	**2,31**	**2,38**$^{*)}$	**2,03**
*) elements with a width of lamellas b=230 mm in the longitudinal layers and b=115 mm in the cross layers; influence has to be evaluated					

A shear strength value of 2,21 N/mm² could be computed (mean strength value: 2,62 N/mm²; COV: 6%, see table 3) with bold values in table 5 for series A and B. Shear in y-direction was dominating, whereas a mean stress level of about 85% developed in x-direction. Test specimens acc. to series C had grooves similar to test specimens of Mestek, but in a less dominant implementation (see Fig. 6.1). As a consequence the strength reduction is quite moderate (9%).

The proposed strength value of 2,21 N/mm² - a similar value can be calculated with data from Mestek - is only valid if stress computation is based on a pure elastic method and rolling shear stresses have to be verified in the vicinity of concentrated load introduction. In bending test according to the usual standards (e.g. EN 16351) the characteristic rolling shear strength is significantly lower (for spruce: $f_{v,k,90}$=1,25

N/mm²). The differences can be explained by the definitely non-linear stress strain behaviour (see following chapter). Therefore the proposed strength values in combination with elastic stress calculation is a simplification for practice.

Bending strength can be checked similarly with forces defined at first crack level (see table 4). Results are summarized in table 6. Values for the specimens of series A are missing as only industrial fabricated panels were tested with test configuration 2.

Table 6. bending strength values (based on results of configuration 2)

Typ of panel	5-layered CLT panel		7-layered CLT panel		
Identification of test series	A_B_5s	B_B_5s	A_B_7s	B_B_7s	C_B_7s
charact. value (EN 14358)	—	203	—	232	280
$m_{x,max}$ [kN·cm/cm]		110,18		61,54	74,27
$m_{y,max}$ [kN·cm/cm]		31,21		69,37	83,72
bending stress σ_x [N/mm²]	—	**30,95**	—	22,17	24,99
bending stress σ_y [N/mm²]	—	22,25	—	**28,52**	**34,72**

Grooves do not influence bending strength significantly. Therefore no differences were made between series B and C. In case of 5-layered CLT element the dominating direction is longitudinal (x) whereas for 7-layered elements the crucial direction is the direction transverse (y). The test results showed that the limiting direction in case of the 7-layered CLT panels does not fit always with the numeric prediction. Mean value over these test results (bold values in table 6) delivers 31,4 N/mm² which is 9% higher than comparable bending strength values of CLT panels ($f_{m,k,CLT}$=1,2·24=28,8 N/mm²). An increase of bending strength can be expected because under a concentrated load only a small area is exposed to high bending moments (volume effect).

7 FE-model for punching shear configuration

It was already mentioned, that a numerical analysis with non-linear behaviour describes mechanical behaviour more precisely than a pure linear-elastic model can do. Such an analysis was carried out with the FE-Software ABAQUS. A solid 3D-model for the 5-layered punching shear configuration '1' was established for one quarter of the test specimen taking into account two planes of symmetry, as shown in fig. 7.1 (a). The numerical model was meshed with linear 3D solid elements 'C3D8'. The first axis of the material orientation denotes the orientation of the lamellas (longitudinal direction), whereas third axis is parallel to the normal direction of the CLT element. Axis 2 is perpendicular to axis 1 and 3 (see fig 7.1 (b)).

The orthotropic MOE parallel to grain was chosen with 12000 N/mm², perpendicular to grain with 370 N/mm². The value of the shear modulus was 690 N/mm² and the rolling shear value 50 N/mm². Stress-strain curves based on data in [12] are shown in fig 7.2 (a). The observed rolling shear behaviour is not ideal elastic-plastic, but this

assumption can be seen as a simplification for the FE-model. The plastic plateau was assumed to be 1,5 N/mm² (see fig 7.2 (a)).

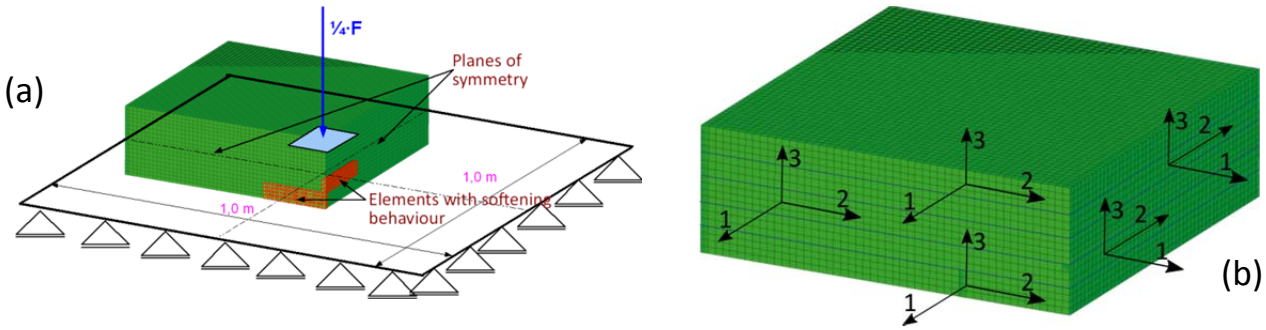

Figure 7.1 (a) FEM Model for punching shear configuration (b) orientations of layers

For simplification all stress-interactions between all stress components were neglected. The orthotropic elastic behaviour and the elastic-plastic behaviour for rolling shear were to be implemented in a user subroutine for ABAQUS. A comparison between computed and experimentally founded load displacement curves can be seen in fig 7.2 (b).

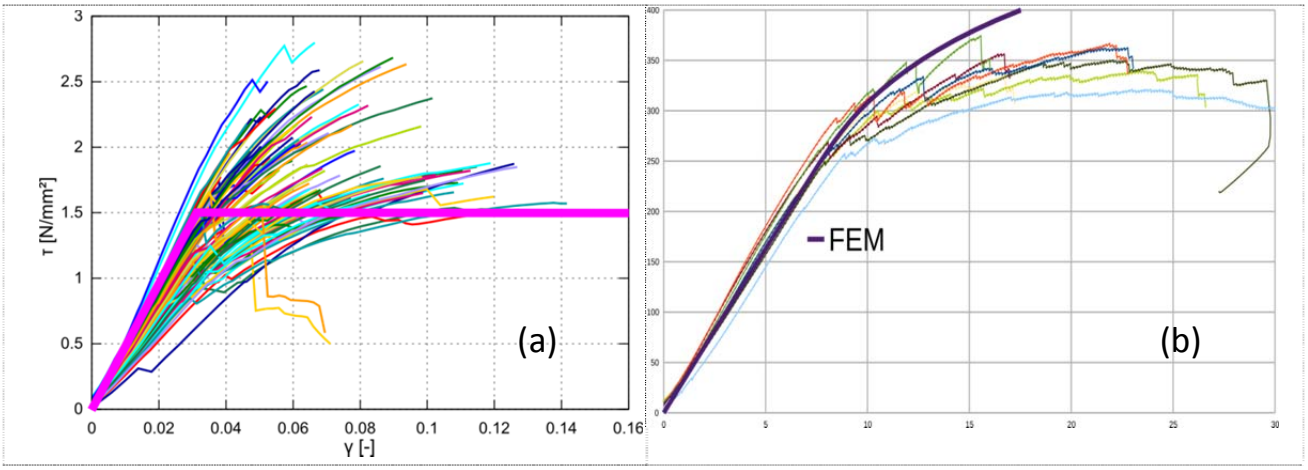

Figure 7.2 (a) stress strain behaviour for rolling shear, based on data of master thesis [12]
(b) FEM results with elastic-plastic behaviour for rolling shear

The agreement is quite pretty good at the beginning where linear elastic behaviour dominates. In the non-linear part (load above 250 kN) the computational model describes behaviour correctly in principal, but overestimates the mechanical strength and resistance of the test specimen. This leads to the conclusion, that another failure mechanism has to be implemented in the model. At the mentioned load level of 250 kN and above significant cracks can be seen in the experimental load displacement curves, which indicates, that softening due to tension in the outer lamellas is missing in the model. This softening behaviour was supplemented in a small domain of the numerical model in two outer lamellas. This domain is highlighted in a red colour and shown in fig 7.1 (a). The size of this selected domain is equal to the height of the outer lamella (34 mm), the width is set to 150 mm. Due to symmetry conditions two lamellas can fail now due to tension in the numeric model in both directions. The location of failure was chosen in the middle of the test specimen, where maximum bending stresses occur. The maximum tension stress, when soften-

ing starts, was introduced with $f_{t,mean}$ =39,0 N/mm². This value bases upon various CLT-bending tests in our laboratory as a mean value. Descend of stress-strain function during softening depends on size of mesh. The area under the stress-displacement curve equals to the fracture energy release rate for Mode I, which was introduced with a value of 1650 J/m², taken from [13]. The complete stress-strain curve with softening is shown in fig 7.3 (a) and added to the user subroutine for ABAQUS. The comparison between computed and experimentally measured load displacement curves is now much better than without softening. Two significant steps in the computed load displacement curve indicates failure in y (m_y) and x (m_x) direction (see fig. 7.3 (b)).

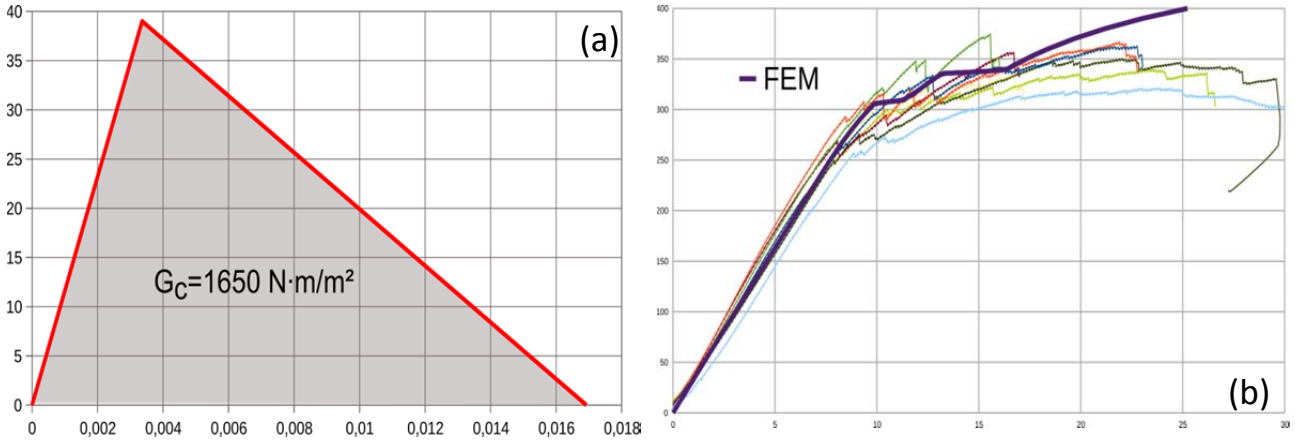

Figure 7.3 (a) stress strain behaviour with softening for outer lamellas under tension (b) FEM results with elastic-plastic behaviour for rolling shear and tension softening in outer lamella

Shown computational results show, that the proposed high strength value of 2,21 N/mm² for rolling shear can be explained by elastic plastic behaviour of rolling shear with some stress redistribution. Further improvements of the numerical simulation could be an implementation of a more precise stress-strain behaviour for rolling shear as well as an implementation of stress interactions, in particular rolling shear with compression stresses perpendicular to grain.

8 Acknowledgement

The research work within the project 'focus_sts' was financed by the competence centre holz.bau forschungs gmbh. The project was financed by funds from the Federal Ministry of Economics, Family and Youth, the Federal Ministry of Transport, Innovation and Technology, the Styrian Business Promotion Agency Association and the Province of Styria (A12), the Carinthian Economic Promotion Fund (KWF), the Province of Lower Austria Department of Economy, Tourism and Technology as well as the Business Location Tirol.

9 References

[1] Bogensperger T. , Silly G., Schickhofer G. (2012): Comparison of Methods of Approximate Verification Procedures for Cross Laminated Timber, Research Report,

holz.bau forschungs gmbh, Institute for Timber Engineering and Wood Technology, Graz University of Technology.

[2] Bogensperger T. , Silly G. (2014): Zweiachsige Lastabtragung von Brettsperrholzplatten, Ernst & Sohn publisher for architecture and technical science GmbH & Co. KG, Berlin. Bautechnik 91 issue 10.

[3] Silly G. (2010): Numerische Studien zur Drill- und Schubsteifigkeit von Brettsperrholz (BSP), diploma thesis, Graz University of Technology.

[4] Bogensperger T. , Wallner B., Augustin M. (2015): Durchstanzen von Brettsperrholzplatten, Research Report to project focus_sts 2.2.3_2, holz.bau forschungs gmbh Graz, (report in progress).

[5] Mestek P. (2011): Punktgestützte Flächentragwerke aus Brettsperrholz (BSP) – Schubbemessung unter Berücksichtigung von Schubverstärkungen, Ph.D., Munich University of Technology.

[6] Jöbstl R. A., Bogensperger T., Moosbrugger T., Schickhofer G. (2006): A Contribution to the Design of Cross Laminated Timber, CIB W18, 39th Meeting, Florence (I)

[7] Schickhofer G., Bogensperger T. , Moosbrugger T. (2009): BSPhandbuch Holz-Massivbauweise in Brettsperrholz Nachweise auf Basis des neuen europäischen Normenkonzepts, Graz University of Technology, 2011, ISBN 978-3-85125-109-8

[8] Peterson, L. A. (2008): Zum Tragverhalten nachgiebig verbundener Biegeträger aus Holz, Berichte des Instituts für Bauphysik der Leibniz Universität Hannover Herausgeber: Univ.-Prof. Dr.-Ing. Nabil A. Fouad; Leibniz Universität Hannover - Institut für Bauphysik Heft 1

[9] Schelling, W. (1982): Zur Berechnung nachgiebig zusammengesetzter Biegeträger aus beliebig vielen Einzelquerschnitten In: Ehlbeck, J. (publisher), Steck, G. (publisher): Ingenieurholzbau in Forschung und Praxis. Bruderverlag Karlsruhe.

[10] Bogensperger T, Augustin M, Schickhofer G. (2011): Properties of CLT-Panels Exposed to Compression Perpendicular to their Plane, CIB W18, 44th Meeting, Alghero , Italy

[11] Mestek P, Kreuzinger H, Winter S (2011): Design concept for CLT - reinforced with self tapping screws, CIB W18, 44th Meeting, Alghero, Italy

[12] Ehrhart T (2014): Materialbezogene Einflussparameter auf die Rollschubeigenschaften in Hinblick auf Brettsperrholz, Masterarbeit, Graz University of Technology.

[13] Mackenzie-Helnwein P. et al (2005): Analysis of layered wooden shells using an orthotropic elasto-plastic model for multi-axial loading of clear spruce wood, Computer methods in applied mechanics and engineering 194, p. 2661-2685